An Efficient Multiscale-Linking Algorithm for Particle Deposition

R. V. Magan and R. Sureshkumar*

Department of Chemical Engineering, Washington University in St. Louis
Campus Box 1198, One Brookings Drive, St. Louis, MO, USA
*Email: suresh@poly1.che.wustl.edu

ABSTRACT

A multiscale-linking computer simulation of irreversible deposition of particles is developed by integrating mesoscopic Brownian dynamics simulations with continuum level conservation laws. The algorithm accounts for the flux of the particles from the bulk suspension into the simulation box by solving the macroscopic mass conservation equation. The location of particles introduced from the bulk into the simulation is derived from the appropriate probability distribution function of the motion of particles using the concept of *probability after effect factor*. This simulation technique is validated for the deposition of diffusing non-interacting particles leading to a monolayer formation. We show that the results for the kinetics and surface structures of the deposit are in full accordance with theoretical and previous simulation predictions.

Keywords: Multiscale, Brownian Dynamics, Monolayer, Colloid Deposition.

1 INTRODUCTION

The deposition of colloidal particles onto solid surfaces is of tremendous importance in many technological applications such as industrial manufacturing, water and wastewater filtration, biofouling of artificial implants, and nanostructured coatings/films. Recently regular arrays of deposited nanoparticles have been proposed as the basis for the design of nanowires and photonic crystals using a 'bottom up' synthesis approach. Numerous experimental studies have shown particle deposition to be typically irreversible and confined to a monolayer for stable colloidal suspensions [1].

Statistical-geometric approaches such as random sequential adsorption (RSA) model have been developed to study irreversible deposition (see [2] for a review). RSA simulations have shown that the maximum fractional surface coverage on a two-dimensional deposition surface, known as the jamming limit coverage, θ_∞, is 0.547 [3]. In RSA the kinetics of deposition are studied by introducing a time scale that is based on the number of attempts to place a particle. For the case of non-interacting hard spheres, Schaaf *et al.* [4] derived an approach to jamming limit by incorporating the surface exclusion effects between adsorbed and free particles, and resulted in a power law of the form $\theta_\infty - \theta = \beta t^{-2/3}$. The RSA model has been further extended to incorporate particle-particle and particle-surface interactions, non-homogeneous deposition surfaces, different shapes of particles and substrates and particle tethering. Despite the advances in incorporating realistic physical phenomena into RSA simulations, they have two inherent limitations: (1) the adsorption of particles is simulated sequentially and (2) the kinetic data obtained do not contain physical time. Moreover, RSA models do not consider the transport of particles beyond a short distance comparable to the particle diameter from the surface. Particle deposition models have also been developed to explicitly consider the transport of particles to surfaces by diffusion and interaction forces based on lattice-based, flux-preserving Monte Carlo simulations [5]. However, similar to RSA models, they are sequential models and cannot predict dynamic effects such as the evolution of surface coverage and deposit structure.

To obtain complete information of the deposition process, non-sequential dynamic simulations need to be performed. An efficient method for the simulation of colloidal systems is the Brownian dynamics simulations (BDS), in which the force imparted on the colloidal particle by the solvent molecules is modeled by a stochastic (Brownian) force. Gray and Bonnecaze [6] developed a BDS technique for monolayer deposition, by considering open simulation boxes and accounting for the flux of the particles into the simulation box based on the probability distribution function of a particle undergoing diffusion in an unbounded medium. For the case of deposition of particles onto a surface, the presence of a deposition surface causes the direction normal to the surface (i.e. the flux direction) to be non-homogenous. Hence a concentration profile develops above the surface leading to a net flux of particles into the simulation volume. Thus in order to perform simulations in boxes with an open top boundary and maintain the correct chemical potential, the flux of particles into the simulation volume must be consistent with those predicted by the continuum-level conservation laws.

In this paper we describe a multiscale-linking algorithm for the simulation of the irreversible deposition of particles. The algorithm couples BDS in a simulation box with an open top boundary, with the solution of the continuum-level conservation law for particle concentration, to incorporate external fluxes from the bulk phase. The algorithm is

applied to the irreversible deposition of diffusing non-interacting hard spheres onto a surface from a quiescent suspension, and the kinetics and deposit structures are compared to previous simulation (RSA) and theoretical results to validate the approach. This algorithm is shown to be computationally efficient as compared to conventional BDS in large simulation boxes with closed boundaries.

2 SIMULATION TECHNIQUE

Simulations are performed in a 3-dimensional simulation box with an open top boundary. The particle trajectories within the simulation box are computed based on the solution of the Langevin equation. In this work, the particle trajectories are based on the Langevin equation adapted for non-interacting diffusing particles [7]. As the particles deposit on the surface, a concentration gradient is developed due to which there is a net flux of particles from the bulk phase into the simulation box. During the course of the simulations, a number of particles are introduced into the simulation box through the open boundary to account for this flux of particles. The number of particles to be introduced in a given time instant is based on the solution of the continuum transient diffusion equation with adaptive Neumann boundary condition. The particles introduced into the simulation box are located appropriately in the simulation box by considering the probability associated with the motion of particles.

Introduction of particles consistent with continuum level conservation laws:

The deposition process under the influence of no external forces can be represented by the transient one-dimensional diffusion equation

$$\frac{\partial C}{\partial t} = D\frac{\partial^2 C}{dz^2} \tag{1}$$

where C is the concentration, D is the diffusion coefficient and z is the direction normal to the surface.

The initial and far-field boundary concentrations are given by

$$C(0,z) = C(t, z\to\infty) = C_0 \tag{2}$$

where C_0 is the bulk concentration.

In order to develop self-consistent BDS, we considered the boundary condition at the surface to be given by the flux at the deposition surface from BDS, $J_s(t)$.

$$-D\frac{\partial C}{\partial z} = J_s(t) \tag{3}$$

The solution of the diffusion equation with non homogenous boundary condition can be obtained by the Duhamels principle as

$$C(z,t) = C_0 + \int_0^t \frac{\exp(-z^2/4D(t-\tau))J_s(\tau)}{\sqrt{D\pi(t-\tau)}}\,d\tau\,. \tag{4}$$

The number of particles introduced into the simulation box, N_{ins}, in a given interval of time from t to $t+\tau$ is given by

$$N_{ins} = Av\times A\int_t^{t+\tau} Flux(t)dt \tag{5}$$

where Av is Avagadro's Number, A is the cross-section area of the top (and bottom) surface, and *flux(t)* is the flux of particles at the top of the simulation box ($z=L$) which is given by

$$Flux(t) = -D\left.\frac{\partial C}{\partial z}\right|_{z=L}\,. \tag{6}$$

During the simulation, the flux of particles at the deposition surface at each time instant τ, $J_s(t)$, is evaluated. At each time instant the concentration profiles in the simulation box is solved for by numerically integrating Eq. 4. The flux of particles at the top of the simulation box is computed from Eq. 6 by implementing a numerical differentiation scheme. The number of particles to be introduced into the simulation box is then computed by Eq. 5.

Location of particles introduced into the simulation box

The particles that are introduced in the simulation box are placed consistent with the probability distribution function for the one-dimensional deposition problem. The probability of finding a particle at a location z_1 at time $t+\tau$, given that it was located at z_2 at time t is given by

$$p(z_1, t+\tau\,|\,z_2, t) = \frac{1}{2\sqrt{\pi D\tau}}\{\exp[-\frac{(z_1-z_2)^2}{4D\tau}] - \exp[-\frac{(z_1+z_2)^2}{4D\tau}]\} \tag{7}$$

The location of a particle, h, in the simulation box is determined by considering the probability of particles in the bulk to be within a location h in the simulation box after time step Δt using the concept of the "*Probability After-Effect Factor" P* introduced by Chandrasekhar [8]. Using the definition of *P,* the probability that a particle will be found within a location h in the simulation box ($0\le z\le h$) in time Δt, knowing that the particle was located outside the simulation box is given by

$$P_h = \frac{1}{2\sqrt{\pi D\Delta t}(H-L)}\int_0^h\{\int_L^\infty[\exp(-\frac{(z_1-z_2)^2}{4D\Delta t}) - \exp(-\frac{(z_1+z_2)^2}{4D\Delta t})]dz_2\}dz_1 \tag{8}$$

The ratio, q, of the probability of a particle to be within a distance h from the surface ($z=0$) to that within the entire simulation box is defined as

$$q = P_h / P_L$$

On substituting from Eq. 8 and after integration

$$q = (\alpha_L+\alpha)\mathrm{erf}(\alpha_L+\alpha) + (\alpha_L-\alpha)\mathrm{erf}(\alpha_L-\alpha) - 2\alpha_L\mathrm{erf}(\alpha_L) + \frac{1}{\sqrt{\pi}}[\exp(-(\alpha_L-\alpha)^2) + \exp(-(\alpha_L+\alpha)^2) - 2\exp(-\alpha_L{}^2)] \tag{9}$$

where $\alpha = \frac{h}{2\sqrt{D\Delta t}}$; $\alpha_L = \frac{L}{2\sqrt{D\Delta t}}$

The location of the incoming particles can be obtained by generating a uniform random number q, $0 \le q \le 1$, and by solving for h from Eq. 9. This gives the z coordinate of the incoming particle, and the x and y coordinates are chosen from a uniform random distribution over the area at the top of the simulation box.

3 RESULTS AND DISCUSSIONS

The simulations were initially repeated for different simulation box heights, and it was found that consistent results are obtained for L=40a, where a is the particle radius. The simulation results presented subsequently represent an average over 8 stochastic simulations performed using different seeds to the random number generator. In these results, time has been made dimensionless according to $\bar{t} = Dt / a^2$.

Kinetics of irreversible monolayer deposition

The kinetics of monolayer deposition were simulated for five different bulk volume fraction, φ, ranging from 0.0025 to 0.05 and the results are shown in Figure 1. The kinetics profiles obtained have the same trend irrespective of φ. The fractional surface coverage, θ, increases rapidly with time at the beginning and slowly at the end when it reaches saturation. It can be seen from Figure 1, that the saturation is reached earlier for the higher φ. The kinetics of the process can be examined in more detail in their small and long time limits.

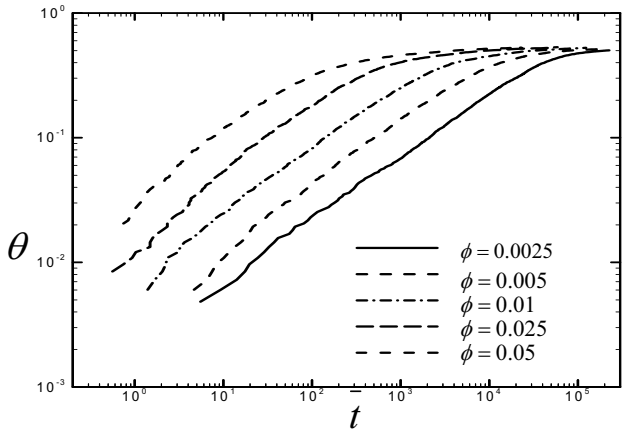

Figure 1: Kinetics of monolayer deposition: Evolution of fractional surface coverage, θ, for different bulk volume fraction φ

Initially when the surface is bare, the particle will deposit easily. However as time increases and more particles have deposited onto the surface, the particles that arrive at the surface may not deposit due to the reduced available surface area. Hence at short times, when there is no hindrance for particle deposition, the deposition surface behaves as a perfect sink (C=0 at z=0). By solving the unsteady diffusion equation (Eq. 1) with the perfect-sink boundary condition, it can be shown that θ increases with square root of time [6]. Figure 2a shows the short-time kinetics for simulations with the different φ. It is observed that the short time kinetics indeed do follow a square root of time dependence.

At long times, saturation in the surface coverage is observed. Particles from the bulk will periodically bombard the surface, and they will deposit when they will be able to find enough free space. Schaaf *et al.* [4] predicted a power law for the long-time kinetics i.e. $\theta_\infty - \theta = \beta t^{-2/3}$. In Figure 2b, we plot θ against –2/3 power of time, and a good linear fit is observed for all the volume fractions. From these plots, we could recover the jamming limit coverage, θ_∞, for our simulations. In these simulations we obtained jamming limit coverage of 0.542-0.546, which is close to the jamming limit coverage of 0.547 obtained from RSA [3]. The long-time kinetic coefficient, β, decreases with φ in a power law fashion (inset in Figure 2b)

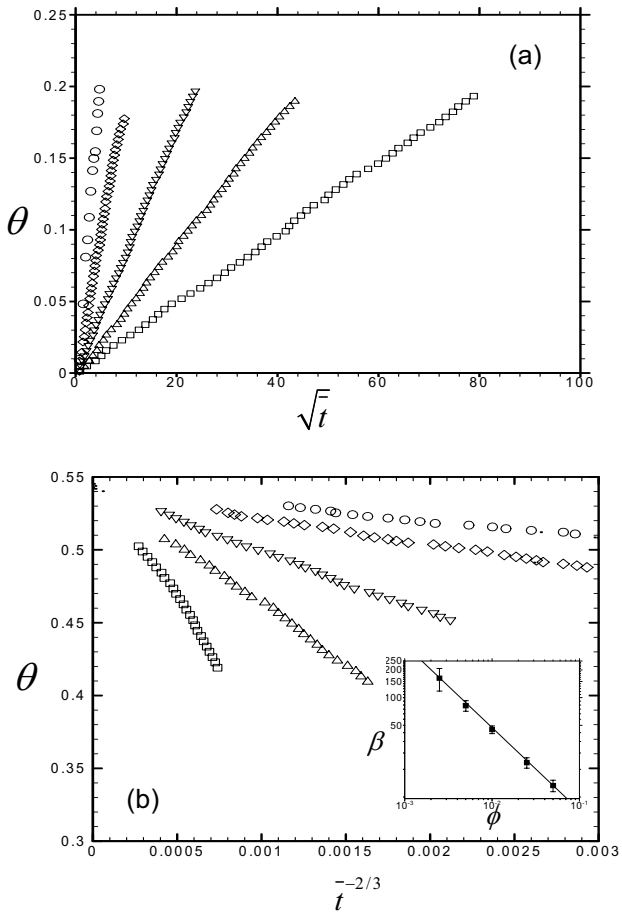

Figure 2: (a) Short time and (b) Long time deposition kinetics for φ =0.0025 (□), φ =0.005 (△),φ =0.01 (▽), φ =0.025 (◇) and φ =0.05 (○). Inset in Figure 2b shows influence of φ on long-time kinetic coefficient β.

Structure of Monolayer Deposits

The structure of the deposited particles is characterized by the radial distribution function, *g(r)* [9]. The evolution of *g(r)* is shown in Figure 3 for $\varphi=0.05$. For small θ values, *g(r)* deviates slightly from unity for all separation distances, indicating that the particle distribution is nearly random. As θ increases, *g(r)* displays an oscillatory nature for short separation distances, with a considerable peak at separation distances equal to the particle diameter. The intensity of this peak increases with increase in θ. The shape of *g(r)* indicates that only a short range ordering is present in the monolayer deposit. This is demonstrated by the fact that $g(r)\rightarrow 1$ for $r/2a>3$. The trends in *g(r)* were the same for the different bulk volume fractions, indicating that volume fraction affects only the kinetics of the deposition. These results for *g(r)* are in good qualitative agreement with those reported from experiments [1] and RSA simulations [9].

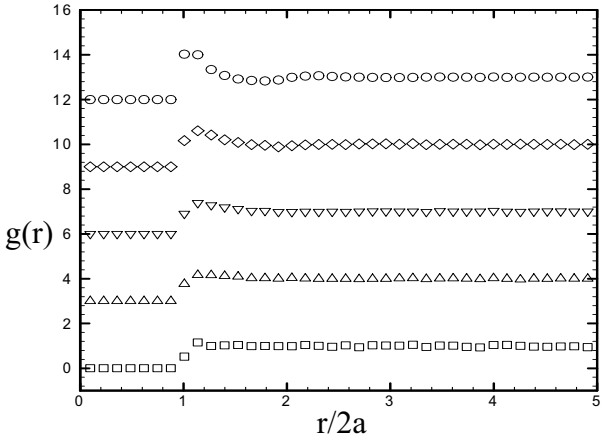

Figure 3: Radial distribution function, *g(r)*, for the deposited layer for $\varphi=0.05$ and $\theta=0.1$ (□), $\theta=0.2$(△), $\theta=0.3$ (▽), $\theta=0.4$ (◇) and $\theta=0.5$ (○). Each successive *g(r)* has been shifted by three units.

Comparison of multiscale approach with conventional BDS

In order to test our multiscale approach, we performed conventional BDS for irreversible deposition of particles in large simulation boxes. The algorithm used is traditional BDS [7] in which the top of the box is simulated as a closed boundary. The box height is kept large so that the saturation in deposition surface is obtained with the concentration at the top of the simulation box remaining nearly constant and equal to the bulk concentration. Figure 4 present the results of θ and *g(r)* for $\varphi=0.005$ for the conventional BDS and the multiscale-approach. These results are in remarkable agreement, thereby validating the multiscale approach of using small simulation boxes with the incorporation of external flux. The key difference between these simulations is the computational time, with the multiscale linking approach being faster by a factor of 5.

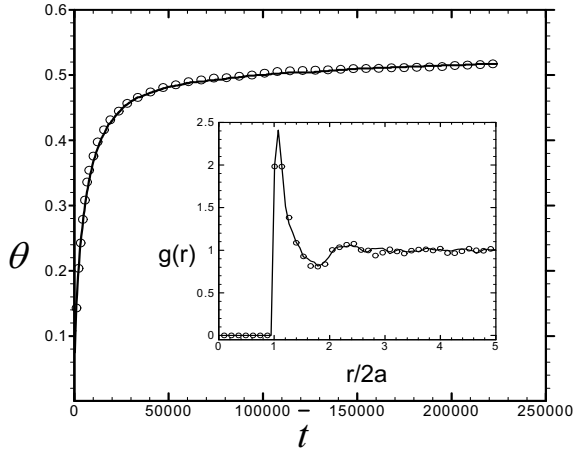

Figure 4: Comparison of evolution of θ and *g(r)* (inset) of the simulations performed with multiscale approach (solid line) and conventional BDS (○) for φ=0.005.

4 SUMMARY

In this paper, a self-consistent multiscale-linking BDS approach was developed to study irreversible deposition processes. The approach has been validated for the simulation of deposition of diffusing hard spheres. Excellent agreement for the kinetics of monolayer deposition with theoretical predictions in the limit of short and long time was obtained. The deposit structure was characterized by the radial distribution function and was found to be qualitatively similar to previous simulation results. The multiscale algorithm was compared to conventional BDS, and statistically indistinguishable results were obtained with smaller CPU times. This approach provides a powerful tool to study colloidal deposition problems under the influence of particle-particle and particle-surface interactions, and external force fields.

REFERENCES

[1] C. A. Johnson and A. M. Lenhoff, J. Colloid Interface Sci., 179, 587, 1996.

[2] P. Schaaf, J. C. Voegel and B. Senger, J. Phys. Chem. B, 104, 2204, 2000.

[3] E. L. Hinrichsen, J. Feder and T. Jossang, J. Stat. Phys., 44, 793, 1986.

[4] P. Schaaf, A. Johner and J. Talbot, Phys. Rev. Lett., 66, 1603, 1991.

[5] P. Kulkarni, R. Sureshkumar and P. Biswas, J. Colloid Interface Sci., 260, 36, 2003.

[6] J. J. Gray and R. T. Bonnecaze, J. Chem. Phys., 14, 1366, 2001.

[7] R. V. Magan, R. Sureshkumar and B. Lin, J. Phys. Chem. B, 107(38), 10513, 2003.

[8] S. Chandrasekhar, Rev. Mod. Phys., 15, 1, 1943.

[9] Z. Adamczyk, P. Weronski, B. Siwek and M. Zembala, Topics in Catalysis, 11/12, 435, 2000.